Journal of Air Transport Management 113 (2023) 102486

Contents lists available at ScienceDirect

Journal of Air Transport Management

journal homepage: www.elsevier.com/locate/jairtraman

An integrated vertiport placement model considering vehicle sizing and queuing: A case study in London

Jose Escribano Macias [a,*], Carl Khalife [b], Joseph Slim [c], Panagiotis Angeloudis [a]

[a] Department of Civil and Environmental Engineering, Imperial College London, South Kensington, SW7 2BZ, London, UK
[b] Bain & Company, Villiers House, 40 Strand, London WC2N 5RW, UK
[c] HSBC, Unit 8, Canada Square, London E14 5HQ, UK

ARTICLE INFO

MSC:
00-01
99-00

Keywords:
Vertiport placement
Urban air mobility
Queuing theory
Vehicle sizing

ABSTRACT

The increasing level of congestion and infrastructure costs in cities have created a need for more intelligent and flexible transport systems. Urban Air Mobility (UAM) introduces the third dimension to intra-urban transport at a minimal infrastructure cost, bypassing congestion and providing reliable travel times to users through the provision of air passenger transportation. The performance of UAM systems is highly dependent on vertiport locations, vehicle sizing and infrastructure specifications, which themselves are intrinsically linked. This study takes a holistic approach to UAM network optimisation by considering the inter-relatedness of these decisions in a three-stage algorithm. In the first stage, a linear vertiport placement model with vehicle sizing constraints is developed to determine the optimal vertiport configuration while considering eVTOL performance. The vertiport configuration serves to determine the operational requirements of the aircraft and are incorporated in the vehicle sizing models. The resulting network configuration and vehicle sizing constraints are used as inputs in the infrastructure model, which utilises open network theory to determine the service rate requirements and the allowed loiter and waiting times based on the number of take-off, landing, and charging pads at each vertiport. These stages are executed sequentially through a feedback mechanism, which balances the infrastructure, operational costs as well as passenger waiting times. The algorithm optimises the profitability of the UAM network ensuring all operational constraints are satisfied. A case study based on the hypothetical implementation of UAM in the city of London is presented using Rolling Origin and Destination Survey data to estimate demand patterns. Our results suggest that ignoring vehicle sizing and infrastructure modelling in the network optimisation stage results in infeasible UAM networks. Furthermore, reducing waiting times and loiter times are critical to reduce operational costs of the UAM network, with all optimal configurations yielding waiting times below 5% of the total flight time. The proposed method can be used to plan future UAM developments whilst ensuring operational viability.

1. Introduction

Urban Air Mobility (UAM) as a concept has been pursued by research and industry since the mid-1900s, yet only recently has technology reached the level of maturity required to make urban air travel economically feasible. There is a significant push from industry to develop the UAM market, with approximately $1 billion being invested by September 2018, and over 70 electrical vertical take-off and landing (eVTOL) manufacturers founded.

While UAM includes various operation types, its most promising application is air passenger transportation, which envisions an operational model to serve intra- and inter-urban transportation, as well as short-haul flights that are not sustainable using traditional aviation (Holmes, 2016).

Its potential market size is valued at $2.5 billion and is estimated to increase to up to $500 billion as the market matures (Goyal, 2018).

Recently, several initiatives have launched to develop UAM services. Volocopter and eHang are leading the way towards commercialisation and are expecting their platform to be fully certified in the near future (EASA, 2021). Several other organisations have announced to develop their own air taxi services, including Lilium, Airbus and Joby, among others.

In terms of air traffic management, NASA is currently developing new technology accommodate UAM operations into existing airspace (Chan et al., 2018). EASA in Europe is also actively developing airspace integration systems which are expected to enable the safe integration

* Corresponding author.
E-mail address: j.escribano@imperial.ac.uk (J. Escribano Macias).

https://doi.org/10.1016/j.jairtraman.2023.102486
Received 28 June 2022; Received in revised form 6 September 2023; Accepted 10 September 2023
Available online 18 September 2023

of UAS operations in urban environments in the near future (European Commission, 2021a,b,c).

UAM systems will function as a passenger transport system within a network of vertiports, which are ground infrastructure to facilitate landing and take-off, and also contain storage and charging capabilities. These can be retrofitted into existing infrastructure, thus reducing initial infrastructure investment requirements (Holden and Goel, 2016).

Johnston et al. (2020) reported that achieving a return on invested capital in the UAM market is possible even for small networks, but highlighted that the cost of charging and refuelling will significantly affect the business case. At the same time, the study stresses the importance of ensuring very fast turnaround times to minimise the total operating costs. The paper also highlights the many factors governing turnaround time, including the number of pads at each vertiport, battery capacity, charging rate, length of trips, and the dispatch strategy.

These findings suggest that developing vertiport placement models to determine the optimal configuration of supporting infrastructure, as well as vehicle parameters, is essential in ensuring the viability of UAM systems. Failing to do so will result in network configurations which are infeasible from an operational perspective. For example, neglecting vehicle sizing constraints might lead to network configurations where the operational requirements are not satisfied. Furthermore, ignoring the effects of the number of pads at each vertiport on waiting times might lead to underestimating turnaround times. Despite these relationships having been reported in the literature, our review of the state-of-the-art suggests that a modelling approach that encompasses these elements is yet to be developed (see Section 2).

To address this gap, this paper proposes an approach to designing battery-powered air-taxi networks by considering the optimisation of three inter-related decisions: vertiport locations, vehicle sizing, and infrastructure design. Each decision is captured in a stage, with vertiport locations being determined through a hub-location problem, and infrastructure specification being obtained using Jackson open network theory (Chen and Yao, 2001). An iterative algorithm is developed that solves three stages sequentially, improving the solution through a feedback mechanism that updates problem parameters until an optimal solution is achieved.

Thus, the paper's contribution is threefold:

1. To the authors' knowledge, it is the first study to formulate the UAM network design problem considering the interrelationships between vehicle sizing, vertiport infrastructure and network design.
2. It models vertiport operations using open network theory, instead of relying on network simulation usually found in literature.
3. It presents a computationally efficient solution heuristic that can accommodate large problem instances. A case study based on the hypothetical design of a London UAM system, in which our algorithm shows significant improvement in all metrics compared to our benchmark.

The remainder of the paper is structured as followed. The literature review is presented in Section 2 where the state of the art is analysed. The mathematical model and formulation are described in Section 3, with the final problem formulation defined in Section 4. The case study and results presented in Section 5. Section 6 provides our discussion, and concluding remarks are presented in Section 7.

2. Current approaches in UAM network design

This section reviews the state-of-the-art in the field of UAM vertiport location planning and vehicle sizing. A summary of the literature reviewed is presented in Table 1, highlighting the features unique to our methodology.

2.1. Vertiport location

The vertiport placement problem is generally structured as a facility or hub location problem, in which the geographical position of the hubs is determined to optimise a specific objective. The literature of the facility location problem is extensive (Klose and Drexl, 2005), with one of the first formulations being the p-median problem (Hakimi, 1964). Extensions to the original problem have been proposed for multiple applications (Campbell, 1996), and has been found to provide an adequate framework to model vertiport placement models, as it allows the positioning of hubs to be governed by economical metrics, such as the travel time savings, weighted demand distance, and infrastructure costs.

Approaches that deviate from the original hub location formulation are unable to consider factors relating to the operation, cost, or capacity of the infrastructure (Lim and Hwang, 2019; Rajendran and Zack, 2019; Sinha and Rajendran, 2022).

Within the hub location framework, Holden and Goel (2016) proposed an initial UAM network configuration model applied to Los Angeles and London case studies. A clustering algorithm is used to group the demand into discrete facility candidate locations, and a facility location algorithm is developed to maximise trip coverage. They find that lengthier trip yield the majority of the savings, yet long trips constitute a minority of the total UAM trips. Further analysis is necessary to determine the viability of the UAM business model.

Similar findings are obtained by Daskilewicz et al. (2018), who developed a vertiport model that assumes short-term eVTOL demand is driven by high income car users with large travel times. They identify that the majority of urban UAM trips are below 30 miles long. Their model, however, ignores infrastructure development and operational costs associated with UAM network design. In addition, operational constraints are not evaluated, as vertiports are given unlimited capacity to allow the optimisation not to focus too many ports in areas of large demand.

Wei et al. (2020) incorporates capacity as a limiting factor in vertiport placement. However, their model tends to focus on high-demand areas, and does not consider origin–destination pairs effectively, resulting in concentration of vertiports in only origin or only destination locations, rather than a network that connects origins to destinations.

Wu and Zhang (2021) propose an integrated demand forecast and a hub-and-spoke vertiport placement model. They evaluate how cost-effectiveness, a measure of the benefit to travellers by reducing travel time, varies at different pricing and network structures. Their findings coincide with Holden and Goel (2016), Daskilewicz et al. (2018) and Wei et al. (2020): the majority of UAM trips involve under 30 miles trips for commuting, despite the main benefits of UAM being long-distance trips. This means that the economic viability of the UAM system requires further analysis.

Rath and Chow (2019) presented an uncapacitated p-median formulation to solve the vertiport placement problem for inter-airport trips. Rath and Chow (2019) evaluated two objectives: a revenue maximisation, and a traveller capture maximisation, modelling vertiports as M/M/c queue systems during post-processing to determine the potential market penetration at each port. They documented a key limitation of the previous approaches: the optimal set of skyports that for short term may not be useful for generating long-term revenue. Models considering only travel time savings may not result in optimal designs in the long term, infrastructure/operational cost is a fundamental consideration for UAM network design.

More recently, Willey and Salmon (2021) proposes a single-allocation p-hub median location problem with modifications to consider multi-leg trips and the probability of passenger travel, among other features. They test several heuristic solutions to overcome the computational complexity of the instance. While the model considers different battery ranges and their effect on the network, their approach fails to consider potential waiting and loitering times due to congestion

Table 1
Literature summary.

Focus	Author	Approach	Objective	Features
Vertiport Location	Holden and Goel (2016)	C, EA	WD	Demand aggregation
	Daskilewicz et al. (2018)	EA	TS	Traffic; Demand
	Wei et al. (2020)	EA	WD	Vertiport capacity
	Rath and Chow (2019)	EA	TS	Transfer; Queue post-process
	Wu (2020)	C	TT	Charging; Scheduling
	Lim and Hwang (2019)	C	D	Case Study
	Rajendran and Zack (2019)	C	D	Time Savings
	Willey and Salmon (2021)	H	TT	Grid-based; Travel Demand
	Wu and Zhang (2021)	C	TT	Mode-choice
	Chen et al. (2021)	H	TT	Grid-based; Travel Demand
	Sinha and Rajendran (2022)	C	ED	Time Savings; Demographics
Vehicle Performance	Silva et al. (2018)	–	W	Aircraft layout
	Johnson et al. (2018)	–	W	Aircraft layout
	Kohlman and Patterson (2018)	–	W	Energy source
	Kohlman et al. (2019)	–	C	Battery size
	Kadhiresan and Duffy (2019)	–	W	Aircraft layout
This paper		EA	TS	Queuing; Battery size

Approach: C — K-means clustering, EA — Exact algorithm.
Objective: C — Cost, D — Distance, TT — Travel Time, TS — Travel Savings, WD — Weighted Demand, W — Weight.

at the vertiports, which undoubtedly affects charging requirements at vertiports, and the overall performance of the UAM network.

Chen et al. (2021) develops a Variable Neighbourhood Search-based heuristic is used to determine the location of vertiports in metropolitan areas. A grid-based approach is developed for an uncapacitated single allocation p-hub median problem, this problem however, does not consider the problem of cost of building and operating a vertiport, and the capacity constraints associated with vertiports, including queuing and pad utilisation.

Operational parameters are incorporated to the vertiport placement problem by Wu (2020). The study proposed a two stage model for vertiport placement and operation scheduling problem, where the latter optimises the charging scheduling of vehicles to minimise total delay for all passengers. They estimate that 7% capture compared to ground transport modes. However, as the operations model is executed as a post-process, the algorithm will not produce optimal results.

The aforementioned methods assume shortest path routes between all vertiports, which is a simplification that ignores air traffic effects on the population and the existence of no-fly zones and obstacles. Wang et al. (2022) proposes a grid-partition method that generates a UAM network at different layers, using a k-shortest paths algorithm that seeks to minimise noise pollution, flight efficiency, and flight safety. This network serves as an input to a traffic assignment model (Wang et al., 2023) that employs a parallel simulated annealing method to minimise airspace complexity, in particular at the network nodes where different traffic routes meet. The algorithms are tested using open-source data from Singapore for UAM delivery systems. The authors show that the regions of higher complexity, the vertical links between the layers, is reduced significantly across several time intervals.

To date, no study considers vehicle performance and vertiport infrastructure design and their effects on charging, loitering, and the overall operational and economical viability. As such, the models reviewed in this section could lead to designs with unreasonable operational and energy requirements.

2.2. Vehicle performance specification

This stream of research aims to determine the optimal power and battery requirements for vehicles to sustain operations using a set mission parameters as input, including the flight time requirements and charging time requirements.

Among the most widely employed tools to design air vehicles is NASA's Design and Analysis Rotorcraft (Johnson, 2010), which has already been used to design air-taxi vehicles (Johnson et al., 2018; Silva et al., 2018). Extensions of this tool have been proposed by Sinsay et al. (2012).

Kohlman and Patterson (2018) proposed a cruise depletion rate parameter to encompass all variables affecting the energy performance into a single value. The approach is refined in Kohlman et al. (2019) in order to incorporate relationships with other critical vehicle properties, such as vehicle mass. The new iterative process developed assumes a power loading parameter for each mission segment to determine the battery size that achieves the specified mission requirements. However, their model assumes constant weight even for diesel-powered aircraft, resulting in an overestimation of the energy requirements.

Another vehicle design tool is presented by Courtin and Hansman (2019) that compares the performance of VTOL and STOL (short take-off and landing) aircraft in terms of maximum take-off weight given varying flight ranges and cruise speeds. While higher-fidelity models for the sub-systems is recommended, the authors determine that STOL configurations are advantageous for missions were Take-off and Landing conditions allow for their use.

Brown and Harris (2018) developed a vehicle sizing model focusing on noise emission, power/energy consumption rates, and costs in the context of UAM. They evaluate their models using UAM-based airport transfers in New York City, and conclude that tilt-rotor aircraft are more cost-beneficial than other configurations. Additionally, they show that hovering is a very significant power-intensive flight stage, and must therefore be kept to a minimum for the operational feasibility of the operation.

Deviating from the previous literature, Kadhiresan and Duffy (2019) performed a weight-based optimisation with consideration of range, speed, rotor size, wing loading and battery energy density parameters for 5 eVTOL configurations: helicopters, multi-rotor, tilt-rotor, tilt-wing, and lift & cruise. In this study, weight is used as a proxy of the direct operational cost, and is therefore the main operational parameter to be optimised. Overall, they observe that lift & cruise performs well overall for all missions, with helicopters and multi-rotors excelling in short-distance missions, and tilt-configurations outperforming the others in long-distance flights.

Vehicle performance design is mainly driven by cost, which is dependent on the required levels of cruise and hover specified by the mission profile. Nevertheless, the provision of insufficient supporting infrastructure in the form of vertiports or landing areas may lead to significant loiter times, which require larger battery sizes and greater costs, while also increasing turnaround times.

However, current research does not consider the effect of loiter time to vehicle performance, vertiport placement and costs. These can be estimated using UAM network simulation, which have been developed

Table 2
Variable, parameter and index definitions.

Indices		Sets	
i, j	nodes	V	node set
u	flight segment	U	route segment set
k	vertiport pad type	K	pad set
Link Parameters		**Vehicle Parameters**	
σ_{ij}	driving time from i to j [h]	$s_{p,u}$	specific power [W/kg]
		s_e	specific energy [Wh/kg]
τ_{ij}	flight time from i to j [h]	N	flight cycles [–]
D_{ij}	demand from i to j [–]	m_p	vehicle payload [kg]
η_{ij}	distance from i to j	m_b	battery mass [kg]
Ψ_{iju}	segment power requirement [W]	B_U, B_L	upper/lower battery level bound [%]
		C	battery C-rate [%/h]
l_{iju}	segment power loading requirement [W/kg]	E	battery energy [Wh]
		B	battery capacity [mAh]
ϕ_{iju}	segment travel time [h]	R_r, R_d	recharge/discharge rate [%/h]
ϵ	value of time [£/h] requirement [W/kg]	R	required recharge [%]
		t_r	recharge time [s]
χ	air taxi travel time saving proportion [–]	M	max take-off mass [kg]
		p_{ikl}	probability of changing [–]
Decision Variables			
x_{ij}	Boolean: open or closes link between two vertiports		
o_i	Boolean: open or closes vertiport i		
z_{ij}	Boolean: flight link requirements satisfied		
c_{ik}	Integer: number of servers per type k at vertiport i		
Q_{ik}	arrival rate [–/h]		
P_{0ik}	probability of no queue [–]		
W_{qij}	waiting time of queue q [s]		
λ_{qij}	queue length [–]		

with varying level of detail (Kohlman and Patterson, 2018; Melton et al., 2014; Patterson et al., 2018; Rothfeld et al., 2018).

While metaheuristics can be used to optimise network design from the simulation, the approach will never yield an optimal solution, and an analytical approach is nevertheless required to benchmark the output of the simulation. Furthermore, the simulation speed becomes the limiting factor of the optimisation, which increases as the scope increases in size and complexity.

2.3. Summary

The infrastructure limitations in vertiports (number of charging, take-off and landing pads) suggests that vehicle fleets will experience waiting and loitering during operation, which is limited by the vehicle operating parameters determined through vehicle design. As such, the vertiport placement models that ignore these will yield operationally infeasible network configurations, as well as underestimate the operational costs and fuel expenditures that result from waiting and loitering. While agent-based modelling can be used to model operations in simulation-optimisation frameworks, they lack practicality due to long run times.

The proposed model in Section 3 overcomes the aforementioned limitations through an iterative network design approach, ensuring UAM networks fulfil operational and infrastructure requirements.

3. Problem definition

This paper proposes a problem formulation to design the UAM network given a pre-defined demand intensity, as well as determining the appropriate vehicle battery size and vertiport properties that minimise overall implementation costs. The model is based on a variant of the uncapacitated p-hub location problem, and selects the optimal locations for the vertiports, as well as the connections between the vertiports that operational and the number of take-off, landing, and recharge pads at each vertiport (see Table 2).

The model is presented in three stages as shown in Fig. 1. Section 3.1 describes the vertiport placement model that focuses on selecting the vertiport locations that maximises the travel savings to customers. It is formulated as a p-hub location problem, and ensures that the selected links between the vertiports conform with the operational constraints defined by the aircraft and infrastructure properties.

The flight operation requirements are used as inputs for the vehicle sizing stage, which determines the vehicle battery size as outlined in Section 3.2. The vehicle size and network design serve to calculate the service rate requirements at each vertiport through the infrastructure model outlined in Section 3.3. Utilising open network theory, the congestion at the vertiports is modelled, and the allowed loiter times based on the number of landing, charging and take-off pads throughout the network is calculated.

The stages are executed in sequence, with the infrastructure at vertiports being modified at each iteration until the marginal cost of operating an additional pad outweighs its marginal benefit. The feedback mechanism (see Section 3.4) is utilised to estimate loiter and waiting times which affect the operational constraints of the vertiport placement model, and may modify the UAM network design. Once the solution becomes stable, which is defined as the iteration where neither the vertiport placements, battery sizes, nor vertiport infrastructure are modified, a solution is reached that outlines the optimal state of infrastructure, operational costs and passenger waiting times.

In formulating the problem, the following simplifications were adopted:

Assumption 1. Driving is the main competitor of air-taxi services. Qualitative air-taxi demand studies (Booz Allen Hamilton, 2018; NASA Urban Air Mobility, 2018) found autonomous cars to be the biggest competitor to air-taxi services. As such, the objective maximises the total time saved in the system relative to driving. While it is acknowledged that other forms of public transport correspond to a significant portion of the mode share, the pricing of UAM will limit its use to high income travellers which are more likely to use taxis and other forms of private road mode of travel (Department for Transport Statistics, 2023).

Assumption 2. Trips are only operated when the factored routing distance lies within a specified bound $H_{\min}, H_{\max}$. Vehicles are assumed to fly at a average speed of 200 km/h, in line with existing eVTOL performance metrics including eHang's E216 and Volocopter's Volocity (Conner et al., 2022), and a safety routing factor $\mu = 1.42$ is assumed as specified by Uber (2018).

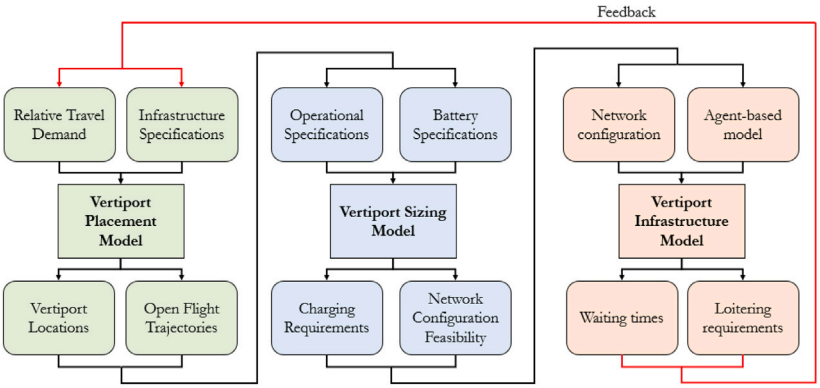

Fig. 1. Solution method workflow. Highlighted in green are the inputs, processes and outputs of the vertiport placement model, in blue the vertiport sizing model, and in orange the infrastructure model. (For interpretation of the references to colour in this figure legend, the reader is referred to the web version of this article.)

Assumption 3. Relative demand levels between vertiports are considered. As German et al. (2018) postulates, absolute demand levels will vary as the service is introduced and are challenging to model. Thus, relative demand levels between the different vertiport locations provide a more accurate depiction of the operational service requirements. Absolute demand capture is dependent of a variety of factors including comfort, travel cost, and user characteristics, which requires conducting a survey and developing a logit choice model. The derivation of accurate absolute demand data is deemed outside of the scope of this study, and the reader is directed to Balac et al. (2019), Fu et al. (2020) and Al Haddad et al. (2020) for detailed studies in this matter.

Assumption 4. The relative demand levels are calculated using (Kohlman and Patterson, 2018)'s distance weighing factor based on existing underground travel data. This represents the typical weekday urban travel behaviour, and is used to estimate air-taxi demand patterns. To represent realistic air-taxi demand levels based on existing transport data-sets, Kohlman et al. (2019) define a distance weighing function, which is calculated based on the haversine distance d as follows:

$$w_d = \frac{1}{367.8791} d^2 e^{-0.001d^2} \tag{1}$$

The distance weighing factor centres demand around distances of 8 to 20 km: trips that are too short or too long to be attractive by air-taxi have been de-emphasised.

Assumption 5. Following Holden and Goel (2016), air taxi trips must provide over 40% travel time savings relative to driving to be considered in the model. Travel time savings constitute the main benefit of UAM. This assumption, alongside Assumption 3, provides reasonable relative levels of demand capture based on existing travel behaviours. Do note that parameter ϕ_{iju} considers flight time during different segments of flight, including take-off and landing.

Assumption 6. The vehicle fleet is composed of eVTOLs Thus, only battery-powered vehicles with recharging capabilities are considered in this problem.

Assumption 7. Each borough can hold at most one vertiport This is consistent with existing studies in the field, where data is aggregated on a census tract level (German et al., 2018; Daskilewicz et al., 2018).

3.1. Vertiport placement model

$$\text{maximise } (\sigma_{ij} - \tau_{ij}) D_{ij} x_{ij} \tag{2}$$

$$\sum_{i \in V} o_i = n \tag{2.1}$$

$$x_{ij} \leq o_j \quad \forall i, j \in V \tag{2.2}$$

$$x_{ij} \leq o_i \quad \forall i, j \in V \tag{2.3}$$

$$z_{ij}\eta_{\min} \leq z_{ij}\eta_{ij} \quad \forall i, j \in V \tag{2.4}$$

$$z_{ij}\eta_{ij} \leq z_{ij}\eta_{\max} \quad \forall i, j \in V \tag{2.5}$$

$$\chi z_{ij}\sigma_{ij} \leq z_{ij}\tau_{ij} \quad \forall i, j \in V \tag{2.6}$$

$$z_{ij} \frac{\sum_{u \in U} \psi_{iju} t_{iju} M + \gamma W_{qi\mathcal{L}}}{m_b} \leq z_{ij} s_{e_{\max}} \quad \forall i, j \in V \tag{2.7}$$

$$z_{ij} s_{e_{\min}} \leq z_{ij} \frac{\sum_{u \in U} \psi_{iju} t_{iju} M + \gamma W_{qi\mathcal{L}}}{m_b} \quad \forall i, j \in V \tag{2.8}$$

$$z_{ij} M \max_{u \in U}(l_{iju}) \leq z_{ij} C_{\max} s_{e,ij} m_b \quad \forall i, j \in V \tag{2.9}$$

$$z_{ij} \frac{Q}{t_r} \leq z_{ij} C_{\max} s_{e,ij} m_b \quad \forall i, j \in V \tag{2.10}$$

$$z_{ij} \frac{\sum_{u \in U} \psi_{iju} \phi_{iju} M}{s_{e_{\max}}} - \frac{E_{\max} - E_{\min}}{N} \leq z_{ij} C_{\max} s_{e,ij} m_b \quad \forall i, j \in V \tag{2.11}$$

$$x_{ij} \leq z_{ij} \quad \forall i, j \in V \tag{2.12}$$

$$o_i, x_{ij}, z_{ij} \in \{0, 1\} \quad \forall i, j \in V \tag{2.13}$$

The objective in Eq. (2) consists of a maximisation of the total travel time savings to customers compared to a private hire road service.

Constraints (2.1)–(2.3) ensure that n vertiports are opened, and only links between opened vertiports are activated. Note that variables o_i, z_{ij} and x_{ij} are set as Boolean by (2.12) and (2.13).

Constraints (2.4)–(2.11) outline the operational conditions that must be met for a link to be usable in the network. Eqs. (2.4) and (2.5) enforce Assumption 2, bounding activated paths by $[\eta_{\min}, \eta_{\max}]$. Constraint (2.6) constitutes Assumption 5, ensuring that links activated provide at least 40% travel time savings with respect to driving.

Constraints (2.7)–(2.11) relate to the vehicle size requirements. The specific energy of the battery must lie within the bounds $s_{e_{\min}}$ and $s_{e_{\max}}$ given (2.7) and (2.8). Finally, (2.8)–(2.11) ensure that the battery size satisfy the charging and discharge requirements for each vertiport i. The origin of these relationships is discussed in Section 3.2.

3.2. Vehicle sizing

This section describes the derivation of the vehicle sizing constraints observed in Eqs. (2.8)–(2.11). The approach developed in this section assumes that 50% of the vehicle mass is attributed to structure and the remaining 50% to battery and payload as informed by Silva et al. (2018). Thus, the maximum take-off mass (M) is expressed as follows:

$$M = 2(m_b + m_p) \tag{3}$$

Determining the battery mass requires the estimation of the operational power requirements. Given a UAM network with specified

connections between vertiports, we ensure operations are feasible for the trip with highest energy requirements as per Eq. (4).

$$G = \max_{ij \in V} \sum_{u \in U} (\psi_{iju} \phi_{iju}) \tag{4}$$

Given a maximum specific energy $s_{e_{\max}}$, which determines the amount of energy produced per unit mass of battery, the minimum battery mass m_b that satisfies the design mission profile is given by (5).

$$m_b = \frac{M \max_{u \in U, ij \in V} (l_{iju})}{s_{e_{\max}}} \tag{5}$$

Rearranging this equation leads to the following expression for battery mass:

$$m_b = \frac{2m_p \cdot \max_{u \in U, ij \in V} (l_{iju})}{s_{e_{\max}} - 2 \max_{u \in U, ij \in V} (l_{iju})} \tag{6}$$

Consequently, the specific energy s_e required to undertake a trip can be written as:

$$s_e = \frac{G}{m_b} \tag{7}$$

Uber's operational requirements (Uber, 2018) states that vehicles must be able to undertake the largest trip in the system for 3 h continuously while only charging for 5 min between trips. This minimises the opportunity costs associated with vehicles servicing less demand due to charging.

Consequently, loiter times would lead to increased recharge rates as the vehicle maintain flight for longer periods. If the recharge rate exceeds to maximum allowable C-rate for Li-Ion batteries, the vehicle will not satisfy Uber's requirement. As such, minimising loiter time not only reduces opportunity costs, but also decreases the peak time requirement for each vehicle. Let us denote E_n before trip n takes place. Considering trip n requires an energy of G_n, after charging E_c, the battery level at E_{n+1} can be defined as:

$$E_{n+1} = E_n - G_n + E_c \tag{8}$$

Let Δt be the duration of one cycle during rush hour, $E_{\min}$ be the required battery level at the end of rush-hour and $E_{\max}$ be the battery level at the beginning of rush-hour. The number of cycles during that window is given by $N = \frac{\Delta t}{T}$ cycles, where T is the time to undertake the largest trip in the system. To reach a desired battery level $E_{\min}$ at the end of rush hour, the required energy recharge R_r is given by:

$$R_r = G - \frac{E_{\max} - E_{\min}}{N} \tag{9}$$

$$E_{\max} = 2(m_b + m_p) s_e B_u \max_{i,j \in V, u \in U} (l_{iju}) \tag{10}$$

$$E_{\min} = 2(m_b + m_p) s_e B_l \max_{i,j \in V, u \in U} (l_{iju}) \tag{11}$$

As the battery discharges rapidly and unpredictably when it falls below its 10% threshold ($B_l = 0.1$), this limit constitutes a lower bound that should never be reached, in addition to any charge reserves required. Furthermore, the top 20% take significantly longer to charge and are usually ignored in UAM models ($B_u = 0.8$) (McDonald and German, 2017). Thus, 30% of the battery capacity is to never be consumed.

The required recharge rate R to satisfy Uber's requirement given a charging time t_r is given by:

$$R = \frac{R_r}{t_r} \tag{12}$$

Li-Ion's batteries dictate the maximum charge/discharge rate a battery can sustain. This is added as a hard constraint in the vertiport placement model. The maximum discharge rate given a battery capacity B is given by:

$$R_d = \frac{2 \max_{i,j \in V, u \in U} (l_{iju})(m_b + m_p)}{B} \tag{13}$$

3.3. Infrastructure specifications

Given a vertiport configuration based on the vertiport location model 3.1, we model each vertiport as an open-network multi-server queuing system using Jackson's theory (Chen and Yao, 2001), which assumes independence of arrival rates at each server in the steady state.

However, waiting times at each pad are not independent of each other in congested scenarios. In practice, congestion will propagate upstream, from storage pads to charging pads, and from charging pads to landing pads. This scenario is infeasible from an operational and service level perspective as loiter times will exceed the predefined battery specifications and passenger waiting times will not be tolerable.

To avoid the aforementioned scenario, the service rate at each pad must exceed the vehicle arrival rate. Assuming a Poisson distributed arrival rate, and a service rate that exceeds arrival rate, a steady state configuration can be reached. In this case, the arrival rates and queue sizes at each server can be assumed to be independent of the other servers in the system.

However, UAM demand is expected to have a bi-modal daily distribution, suggesting that the system will not operate in a steady state configuration. Nevertheless, designing the system to a steady state configuration with a similar behaviour to rush hour conditions will lead to a configuration that is feasible for lower demand levels. Consequently, queuing theory can be used to optimise the number of landing, charging, storage and take-off pads assuming a steady state, rush-hour configuration.

Each vertiport i contains a set of pad types $k \in K$, namely take-off, charging, storage, and landing. We define the arrival rate at each pad type k for each vertiport i during rush hour arrival as Q_{ik}, with the arrival at landing pads for vertiport i denoted as $Q_{i\Gamma}$. Furthermore, each pad type k has a service rate μ_{ik} at vertiport i, as well as a set of probabilities $p_{ikk'}$ for a vehicle in vertiport i to transition to pad type k' from pad type k. The arrival rates at each vertiport $Q_{i\Gamma}$, transition probabilities $p_{ikk'}$ and the service rate μ_{ik} pre-calculated for different network configurations for a very large number of pads at each vertiport, ensuring all demand is satisfied. This enables us to study the behaviour of each vertiport independently. At each vertiport, the vehicles are routed to different pads in a probabilistic manner.

First, the service rate of each server μ_{ik} should exceed the arrival rate Q_{ik} at each pad type k at vertiport i to ensure steady-state conditions. Let c_{ik} be the number of pads of type k at vertiport i, the steady-state condition is given as follows:

$$\frac{Q_{ik}}{\mu_{ik} c_{ik}} < 1 \tag{14}$$

If steady state conditions (14) are not satisfied, the queue size is expected to increase indefinitely, leading to the aforementioned congested scenario. Given an arrival rate $Q_{i\Gamma}$ at the landing pads Γ of vertiport i, the arrival rate Q_{ik} at each pad k of vertiport i is calculated as follows:

$$Q_{ik} = \sum_{k'}^{K} (p_{ik'k}) Q_{i\Gamma} \tag{15}$$

For each pad k of vertiport i, the utilisation ρ_{ik} is defined as:

$$\rho_{ik} = \frac{Q_{ik}}{\mu_{ik}} \tag{16}$$

The probability P_{0ik} of an empty queue at pad k of vertiport i is calculated as follows:

$$P_{0ik} = [\sum_{n=0}^{c-1} \frac{\rho_{ik}^n}{n!} + \frac{\rho_{ik}^{c_{ik}}}{c_{ik}!(1 - \frac{\rho_{ik}}{c_{ik}})}]^{-1} \tag{17}$$

The average length of the queue L_{qik} is given by:

$$L_{qik} = \frac{P_{0ik} \rho_{ik}^c \frac{\rho_{ik}}{c}}{c!(1 - \frac{\rho_{ik}}{c})^2} \tag{18}$$

Finally, the waiting time W_{qik} at pad k of vertiport i is given by:

$$W_{qik} = \frac{L_{qik}}{Q_{ik}} \tag{19}$$

Waiting times directly affect the vertiport placement and vehicle sizing models as per Eqs. (20.7) and (20.8). Wait times reduce the travel time savings relative to driving and overall benefit of the UAM network, while loiter times lead to increased battery size requirements, which can make some trips unfeasible due to the recharge constraints. Larger vehicle size and increased energy depletion due to loiter increase the cost of vehicle procurement, charging and maintenance. Consequently, waiting times heavily influence the operational feasibility of the UAM network and the system costs.

3.4. Feedback mechanism

Increasing the number of landing, charging and storage pads will lead to improve waiting times and reduce opportunity costs provided the requirements are satisfied. Despite these improvements, it will also increase the infrastructure costs.

This interrelationship is captured using a feedback mechanism, which collects the output of the vertiport infrastructure model (vehicle waiting and loitering times, battery recharge capabilities and costs), and updates the constraints of the vertiport placement model based on the requirements of the vertiport infrastructure. In the first instance, the number of pads at each port is large enough to ensure no queuing. At each iteration, the model calibrates the number of take-off, charging and landing pads until one of two conditions are met: (1) the marginal cost of removing a pad exceeds the marginal benefit of doing so, and (2) the operational requirements to operate the UAM network make it infeasible.

4. Full mathematical model

We combine the formulations and derivations presented in the previous section to develop the full mathematical problem shown in equation set (20).

$$\text{minimise } TC - (\sigma_{ij} - \tau_{ij}) D_{ij} x_{ij} \epsilon \tag{20}$$

$$\sum_{i \in V} o_i = n \tag{20.1}$$

$$x_{ij} \leq o_j \quad \forall i, j \in V \tag{20.2}$$

$$x_{ij} \leq o_i \quad \forall i, j \in V \tag{20.3}$$

$$z_{ij} \eta_{\min} \leq z_{ij} \eta_{ij} \quad \forall i, j \in V \tag{20.4}$$

$$z_{ij} \eta_{ij} \leq z_{ij} \eta_{\max} \quad \forall i, j \in V \tag{20.5}$$

$$\chi z_{ij} \sigma_{ij} \leq z_{ij} \tau_{ij} \quad \forall i, j \in V \tag{20.6}$$

$$z_{ij} \frac{\sum_{u \in U} \psi_{iju} t_{iju} M + \gamma W_{i\mathcal{L}}}{m_b} \leq z_{ij} s_{e_{\max}} \quad \forall i, j \in V \tag{20.7}$$

$$z_{ij} s_{e_{\min}} \leq z_{ij} \frac{\sum_{u \in U} \psi_{iju} \phi_{iju} M + \gamma W_{i\mathcal{L}}}{m_b} \quad \forall i, j \in V \tag{20.8}$$

$$z_{ij} M \max_{u \in U}(l_{iju}) \leq z_{ij} C_{\max} s_{e,ij} m_b \quad \forall i, j \in V \tag{20.9}$$

$$z_{ij} \frac{Q}{t_r} \leq z_{ij} C_{\max} s_{e,ij} m_b \quad \forall i, j \in V \tag{20.10}$$

$$z_{ij} \frac{\sum_{u \in U} \psi_{iju} \phi_{iju} M}{s_{e_{\max}}} - \frac{E_{\max} - E_{\min}}{N} \leq z_{ij} C_{\max} s_{e,ij} m_b \quad \forall i, j \in V \tag{20.11}$$

$$x_{ij} \frac{D_{ij}}{\zeta} \leq n_{ij} (\tau_{ij} + \sum_{k \in K} W_{i,k} + t_r) \quad \forall i, j \in V \tag{20.12}$$

$$f(\sum_{j \in V} n_{ji}) \leq Q_{in} \quad \forall i \in V, \ \forall k \in K \tag{20.13}$$

$$\frac{Q_{ik}}{\mu_{in} c_{in}} < 1 \quad \forall i \in V, \ \forall k \in K \tag{20.14}$$

$$g(Q_{ik}) \leq W_{ik} \quad \forall i \in V, \ \forall k \in K \tag{20.15}$$

$$x_{ij} \leq z_{ij} \quad \forall i, j \in V \tag{20.16}$$

$$o_i, x_{ij}, z_{ij} \in \{0, 1\} \quad \forall i, j \in V \tag{20.17}$$

$$c_{ik} \in Z^+ \quad \forall i \in V \ \ \forall k \in K \tag{20.18}$$

$$Q_{ik}, W_{ik} \in R^+ \quad \forall i \in V \ \ \forall k \in K \tag{20.19}$$

The objective is outlined by Eq. (20), which minimises the total cost TC of the UAM system and maximises total travel time savings for customers. The cost function is described in greater detail in equation set (21).

Constraints (20.1)–(20.11) are analogous to those shown in (2.1)–(2.11), where (20.7)–(20.11) relate to the vehicle size requirements derived in Section 3.2. Variables o_i, z_{ij} and x_{ij} are set as Boolean by (20.17).

The remaining constraints (20.12)–(20.15) determine the appropriate vertiport design in terms of number and type of pads at each selected location and are derived in Section 3.3. Constraint (20.12) determines the number of vehicles to be utilised for each connection, which must meet the frequency of flight required based on the demand intensity between each station. Eq. (20.13) defines the arrival rate of vehicles at each vertiport as a function of the number of vehicles assigned to each link. Constraint (20.14) ensures the queue at vertiport i is steady, meaning that the queue size will not increase indefinitely. Constraint (20.15) relates the arrival rate with the total waiting time at each vertiport and pad. Finally, constraints (20.18)–(20.19) set c_{ik} as a positive integer, and Q_{ik} and W_{ik} as positive real numbers.

The total costs TC in the objective function is comprised of nine elements: maintenance costs, vehicle acquisition and insurance costs, pilot salary, energy expenditure costs, battery acquisition and maintenance costs, indirect costs, opportunity costs, and infrastructure costs.

Maintenance costs and pilot salaries are calculated based on the hours flown by each vehicle respectively. Vehicle acquisition and insurance costs are a function of number of vehicles in the UAM network. Energy and battery acquisition costs, as well as carbon tax, are calculated based on the total energy requirements of the network. Indirect costs include credit card fees, overhead from commercial aviation, taxing, landing fees and others and are modelled as a percentage of maintenance, energy costs, vehicle and battery procurement costs, and carbon tax. Finally, opportunity costs are calculated based on the proportion of waiting time from the total trip time.

The main infrastructure cost components are associated with the acquisition of land, and the development of landing, charging, storage, and takeoff pads. The latter includes the cost of piling, composite decking as well as the carrier terminal cost. These costs are used to determine the infrastructure cost of different vertiports deployment scenarios. Additionally, a high voltage charger cost of is included for each charging pad. The take-off and landing pads for eVTOL vehicles are comparable to a helicopter pad.

These relationships are expressed using a parameter for each cost type ($\mathcal{M}$, $\mathcal{V}$, $\mathcal{C}$, $\mathcal{E}$, $\mathcal{B}$, $\mathcal{T}$, $\mathcal{O}$, $\mathcal{D}$, $\mathcal{I}$). The values and reference for each parameter are outlined in Table 3 in Section 5.

$$TC = MC + VC + CC + EC + BC + CT + OC + DC + IC \tag{21}$$

$$MC = \mathcal{M} \sum_{i,j \in V} (\sum_{i,j \in V} W_{i\mathcal{L}} + \sum_{u \in U} \phi_{iju}) \tag{21.1}$$

$$VC = \sum_{i,j \in V} n_{ij} \mathcal{V} \tag{21.2}$$

$$CC = \sum_{i,j \in V} n_{ij} \mathcal{C} \tag{21.3}$$

$$EC = M\mathcal{E} \sum_{i,j \in V} (\gamma W_{i\mathcal{L}} + \sum_{u \in U} \psi_{iju}) \sum_{i,j \in V} x_{ij} n_{ij} \tag{21.4}$$

$$BC = M\mathcal{B} (\sum_{i,j \in V} \gamma W_{i\mathcal{L}} + \sum_{u \in U} \psi_{iju}) \sum_{i,j \in V} x_{ij} n_{ij} \tag{21.5}$$

Table 3
Cost parameters.

Parameter	Value	Reference
Operating costs		
Mechanic salary [$/h]	60	Booz Allen Hamilton (2018)
Maintenance time [h]	0.68	Booz Allen Hamilton (2018)
Vehicle acquisition [$/kg]	333	Booz Allen Hamilton (2018)
Pilot salary [$/h]	100	Brown and Harris (2018)
Pilot yearly flight-hours [h]	500	Booz Allen Hamilton (2018)
Energy costs [$/MJ]	0.0492	PowerCompare (2019)
Emissions rate [kg/MJ]	0.0786	Kohlman et al. (2019)
Battery acquisition [$/MJ]	111	Booz Allen Hamilton (2018)
Carbon tax [$/kg]	0.0198	HM Revenues and Customs (2018)
Operating margin [–]	0.3	Johnston et al. (2020)
Infrastructure costs		
Vertiport costs [$/m^2]	4782	Turner & Townsend (2015), Taylor et al. (2020), Fixr (2021), Ministry of Housing Communities & Local Government (2020)
High-voltage charger [$]	453	Holden and Goel (2016)

$$CT = M\mathcal{T}\Big(\sum_{i,j\in V}\gamma W_{i\mathcal{L}} + \sum_{u\in U}\psi_{iju}\Big)\sum_{i,j\in V}x_{ij}n_{ij} \tag{21.6}$$

$$OC = \mathcal{O}\sum_{i,j\in V}(\tau_{ij}\sum_{k\in K}W_{ik}) \tag{21.7}$$

$$DC = \mathcal{D}(MC + IC + CC + EC + BC) \tag{21.8}$$

$$IC = \sum_{k\in K, i\in V}\mathcal{I}_k c_{ik} \tag{21.9}$$

5. Case study

The method described in Section 3 is applied to find the optimal system configuration for a potential deployment scenario in the city of London. This study assumes a five vertiport configuration for the short-term UAM application. To showcase the study's contribution, a base-line model based on the current literature is developed which ignores the interdependencies between vertiport placement, vehicle sizing and infrastructure specifications. This baseline is used as a comparison to the integrated approach proposed in this paper. All cost parameters are presented in Table 3.

The problem is solved using a desktop computer with 256 GB RAM, and an i9-i010980XE processor. The solution method described in the previous section is implemented in Python 3.6, and the vertiport placement model is solved using Gurobi 9 through the Python package PuLP.

5.1. Demand generation

As stated by German et al. (2018), UAM is still in its early stages of development to forecast absolute demand levels for trips within a city. However, using existing transportation data, one can estimate relative demand levels between the different possible vertiport locations.

As per Assumption 4 in Section 3, we utilise TfL's Rolling Origin and Destination Survey (RODS) data based on November 2017 (Transport for London, 2019). While previous studies identify high-income individuals as the main users of UAM, which are more likely to use taxis, research has also found that commuting is the main reason for UAM transportation, which RODS captures well. Additionally, high-income individuals in the UK use the London Underground service and National Rail to higher rates than lower income groups (Department for Transport Statistics, 2023). Furthermore, note that these values are relative demand levels, essentially developing attraction and production rates in each region.

We aggregate the demand to a borough level, resulting in the candidate locations outlined in Fig. 2 and Table 4. One limitation of this approach is that the boroughs of Bexley, Bromley, Croydon, Kingston upon Thames and Sutton, which are not served by underground stations, will not have demand associated to them.

The final relative demands are calculated by applying (Kohlman and Patterson, 2018) distance weighing factor (1)

5.2. Results

The baseline model developed for this study is defined by Eqs. (20)-(20.6) and (20.16)–(20.18) and represents a linear vertiport location model with a predefined maximum flight range. This is a common approach in the current literature, which undertake additional analysis of the vertiport locations during post-processing.

Our model proposed in Section 3 is also used to incorporate the effects of waiting times and vehicle performance into the original vertiport placement model, as well as determining the optimal pad configuration at each vertiport. An initial upper boundary pad configuration of 16 pads per vertiport is used to ensure operational feasibility. This value is determined from pre-analysis, and ensures a steady queue regardless of demand intensity.

This number is reduced until the marginal cost of removing a certain pad outweighs the marginal benefit of doing so, provided the operational constraints are satisfied. To quantify the effects of increasing demand on the system, the model is run for seven rush-hour demand scenarios, denoted as follows: L, ML, M, MH, H, VH, E for 50, 100, 150, 200, 250, 300 and 350 vehicles/h, respectively.

All demand scenarios lead to the same optimal vertiport configuration and vehicle size (see Fig. 4). In comparison to the baseline model the longest trip in the system is 39% shorter, that being the 14 km trajectory connecting Barnet to Westminster. The baseline selects the Brent-Newham connection of 23 km as its longest trajectory. It is interesting to note that the proposed approach yields a configuration that seems reduces connections to the west and south of London. This is mainly for the following reasons: including vertiports on the south and east will lead to significantly longer and operationally infeasible flight routes, thus eliminating the direct connection and travel time savings between peripheral stations. Furthermore, the west and south contain less demand, one can see in Fig. 3 that the east contain the majority of demand connections to the centre most likely due to the presence of City Airport, which is regularly used for business trips.

In spite of the shorter travel distances, the battery size in the proposed model is 6% larger than in the baseline case. This suggests that the vehicle sizing model is unable to produce a feasible battery size for this trip, highlighting a key limitation of existing methods.

Fig. 5 highlights that, although both vehicle configurations are effectively able to fly the largest trip in the system, the baseline configuration does not satisfy Uber's operational requirements under reasonable C-rate assumptions. In fact, battery levels deplete below reserve after only undertaking 2 trips while charging at a 5C rate. The proposed model provides sufficient capacity to undertake the longest

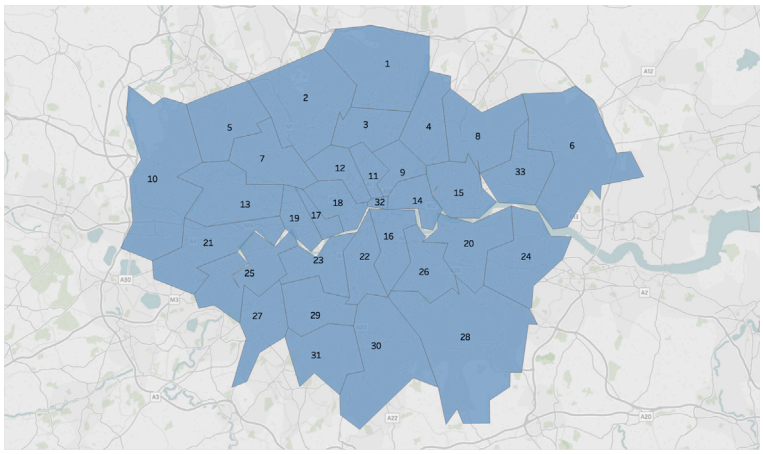

Fig. 2. London borough map.

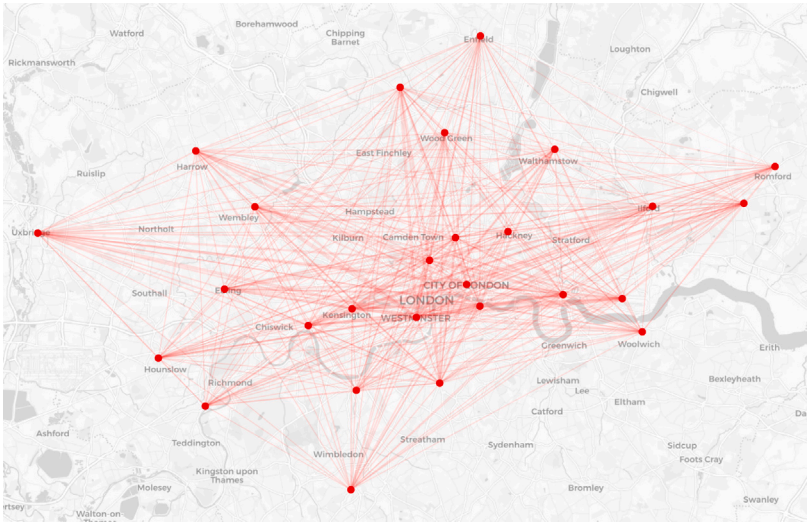

Fig. 3. London RODS demand weight map.

Table 4
Borough candidate vertiport location. WF: Waltham Forest, K&C: Kensington and Chelsea, H&F: Hammersmith and Fulham, RUP: Richmond-upon-Thames, KUP: Kingston-upon-Thames, B&D: Barking and Dagenham, TH: Tower Hamlets, COL: City of London.

ID	Borough	Latitude	Longitude	ID	Borough	Latitude	Longitude
1	Enfield	51.6538	−0.0799	18	Westminster	51.4973	−0.1372
2	Barnet	51.6252	−0.1517	19	H&F	51.4927	−0.2339
3	Haringey	51.6000	−0.1119	20	Greenwich	51.4892	0.0648
4	WF	51.5908	−0.0134	21	Hounslow	51.4746	−0.3680
5	Harrow	51.5898	−0.3346	22	Lambeth	51.4607	−0.1163
6	Havering	51.5812	0.1837	23	Wandsworth	51.4567	−0.1910
7	Brent	51.5588	−0.2817	24	Bexley	51.4549	0.1505
8	Redbridge	51.5590	0.0741	25	RUP	51.4479	−0.3260
9	Hackney	51.5450	−0.0553	26	Lewisham	51.4452	−0.0209
10	Hillingdon	51.5441	−0.4760	27	KUP	51.4085	−0.3064
11	Islington	51.5416	−0.1022	28	Bromley	51.4039	0.0198
12	Camden	51.5290	−0.1255	29	Merton	51.4014	−0.1958
13	Ealing	51.5130	−0.3089	30	Croydon	51.3714	−0.0977
14	TH	51.5099	−0.0059	31	Sutton	51.3618	−0.1945
15	Newham	51.5077	0.0469	32	COL	51.5155	−0.0922
16	Southwark	51.5035	−0.0804	33	B&D	51.5607	0.1557
17	K&C	51.5020	−0.1947				

trip in the system continuously for 3 h while only charging for 5 min at a 4.8 C-rate.

With notion of the effects of the pad configuration on waiting times, and hence operational costs, the proposed model can also be used to determine the optimal pad configuration at each vertiport (see Fig. 6).

The yearly operational cost ranges between $280 million and $40 million between the largest and lowest demand instances E and L. The increment in operational cost is linear throughout, with battery, vehicle maintenance and crew costs comprising the largest proportion of the expenses.

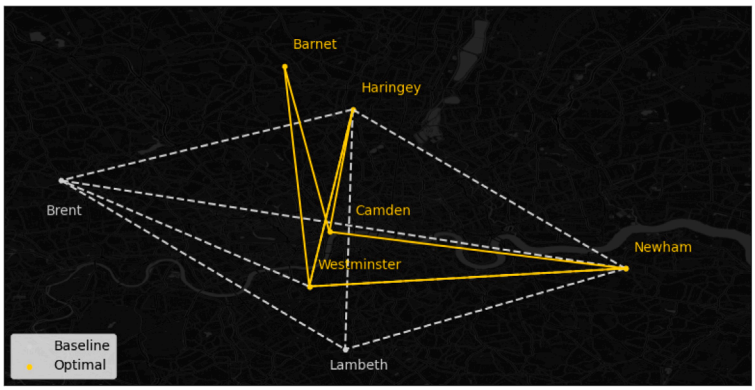

Fig. 4. Vertiport placement results for the baseline and optimal case. Haringey, Westminster and Newham are selected in both cases.

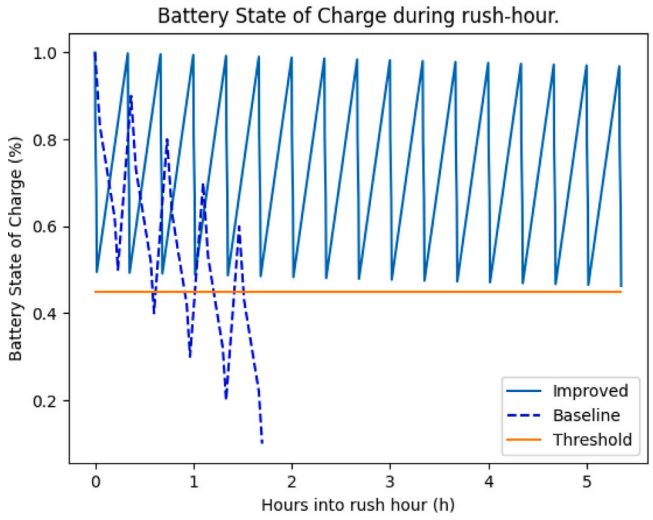

Fig. 5. Battery state of charge variation during peak-time.

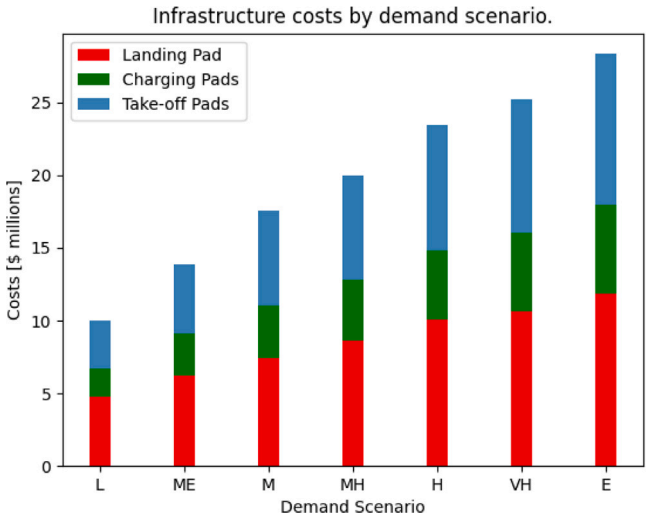

Fig. 7. Infrastructure costs for each demand scenario.

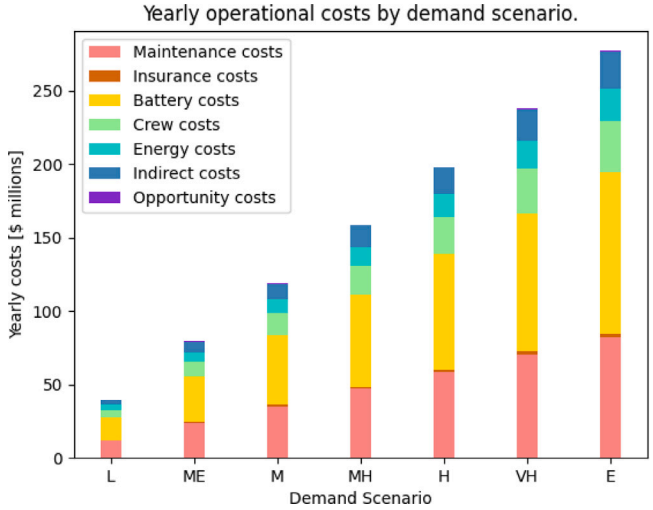

Fig. 6. Yearly operational costs.

Due to the Li-Ion's battery life and price ranges, the battery costs are the highest operational cost component, which is in line other studies (Johnston et al., 2020). Improvements in battery performance thus offers significant cost reduction opportunities. Booz Allen Hamilton (2018) assumption of 33 min per flight hour for maintenance makes associated costs significant. Further, automation has the opportunity to eliminate pilot costs, but will lead to additional costs which should be quantified.

Similar to operational costs, infrastructure costs also increase linearly with demand as a result of the larger infrastructure requirements, from $10 million in the lowest demand case, to $28 million in the highest demand scenario (see Table 5). Interestingly, a larger number of charging pads are required compared to the other types under all conditions. This makes intuitive sense due to the longer service time of charging pads. Further, there are more landing pads than take-off pads in all scenarios, suggesting that marginal cost of removing a landing pad is larger than the one associated with removing a take-off pad (see Fig. 7).

In fact, the model reduces waiting and loitering times for all demand scenarios, maintaining them below 5% of the total flight time in all optimal configurations, and in most cases, it is kept below 1%. Waiting times increase opportunity and maintenance costs considerably, leading to greater marginal costs that out weight the benefit of removing a vertiport pad. Loitering times have a significant effect on energy requirements, which not only increases charging times and costs, but also may result in an infeasible rush-hour service as highlighted by Fig. 5. Fig. 8 shows how marginal profit changes with decreasing number of landing pads, and shows how loitering times greater than 5% of the total flight time result in economically infeasible UAM networks.

Note that operating costs are orders of magnitude larger than infrastructure costs in both scenarios, strengthening the notion that,

Table 5
Vertiport infrastructure requirements and costs.

Scenario	L	ML	M	MH	H	VH	EH
Landing Pads [–]	16	21	25	29	34	36	40
Charging Pads [–]	16	23	29	34	38	43	49
Take-off Pads [–]	11	16	22	24	29	31	35
Waiting Time Proportion [%]	3.16	1.27	0.82	0.57	0.41	0.64	0.42
Infrastructure Costs [$ million] (% of total)							
Landing Pads	4.75 (47)	6.22 (44)	7.42 (42)	8.60 (43)	10.09 (43)	10.67 (42)	11.86 (42)
Charging Pads	1.99 (20)	2.87 (21)	3.60 (21)	4.24 (21)	4.72 (20)	5.37 (21)	6.12 (22)
Take-off Pads	3.27 (33)	4.74 (34)	6.53 (37)	7.12 (35)	8.61 (37)	9.19 (36)	10.38 (37)
Total	10.01	13.84	17.55	19.96	23.42	25.23	28.35

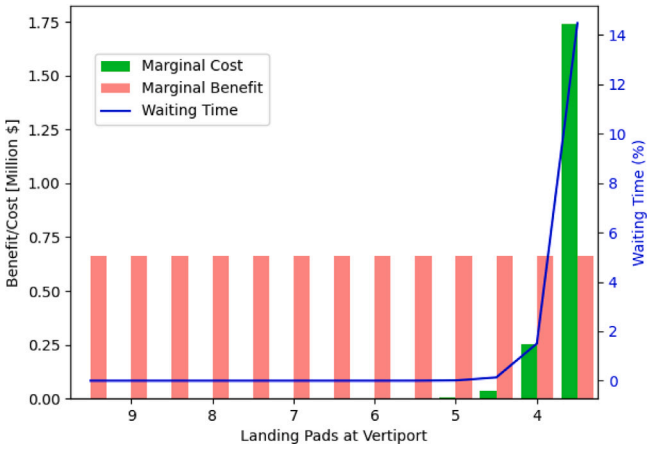

Fig. 8. Marginal costs and total vehicle waiting times with number of landing pads at scenario L (50 veh/h).

if retrofitted into existing infrastructure, UAM offers significant cost advantages compared to other transport modes.

6. Discussion

The study demonstrates the importance of adopting a holistic approach to UAM network design. Its major contribution lies in the development of a method that optimises the main components of UAM systems, while also considering the inter-dependencies between them. By integrating vehicle sizing and performance constraints into the vertiport placement model, the proposed methodology generates a vertiport configuration that satisfies Uber's peak time requirements of undertaking 3 h of continuous operation at peak time with only 5 min recharge in-between trips.

In contrast, the baseline model yields an infeasible solution that is only detected during post-processing. A potential solution is to reduce the number of opened links between the network in order to reduce the peak demand at the vertiports, but this solution will result in a suboptimal UAM network.

Our results show that under low waiting times, battery acquisition and replacement cost are the largest operating cost component. Nevertheless, opportunity costs quickly dominate when waiting times increase, making UAM networks unsustainable. Thus, UAM operations should be designed to operate under minimal turnaround times.

Another interesting insight is that operating costs grow at a faster rate than infrastructure costs when waiting times increase. Therefore, it is advisable to design vertiports to accommodate near 0 theoretical average waiting times at rush-hour. Loiter times lead to the largest increases in operational costs. Not only do they lead to opportunity cots, but they also deplete additional energy, therefore requiring larger batteries and larger charging times.

Sub-system level interactions largely affect the wider UAM network. Increases in waiting times lead to changes in network configuration, operating costs and battery requirements which can make the system unfeasible. Waiting times are heavily dependent on the configuration of pads at each vertiport. Consequently, feedback loops can be used to model the effects of sub-system interactions on the wider UAM system to a reasonable degree.

In spite of these findings, there are several limitations with the approach in this study. The demand modelling is on RODS (Transport for London, 2019) which only consider trip undertaken in the London Underground. The model can be improved by considering other modes of transport and including a logit decision model based on the utility parameter of each mode (Fu et al., 2020). This includes analysing the effects of different pricing schemes in UAM demand as well as queue management.

Furthermore, multi-mode trips, where UAM can be used to complement existing transport modes, are ignored in this study. The safety routing factor *mu* specified in Assumption 2 simplifies the potential effects of air traffic management and noise in the routing of eVTOLs and the configuration of vertiports. Finally, incorporating stochastic travel times, waiting times, and demand levels would provide a more robust network, particularly when incorporating weather effects on demand and flight times.

Nevertheless, the model can be utilised to plan future UAM development ensuring operational viability. For instance, one can estimate air-traffic flows between the vertiport locations and estimate the workload on the civil aviation authority. This analysis can be used to determine the level of safety required for this operation, as well as assessing the potential health impact on residents caused to noise pollution. The outcomes of such studies should inform future regulation of UAM operations.

7. Conclusions

This study proposes a holistic approach to optimising UAM networks by considering sub-system interactions on the wider UAM network. The methodology contains three main components: a vertiport placement model, a vehicle sizing process, and a infrastructure queuing model. The latter can be modelled using multi-server open network theory by considering a rush-hour, steady state demand configuration, and its outputs are used to modify the constraints of the vertiport placement model. This approach overcomes the speed limitations related to simulation-optimisation approaches that could be used with the existing agent-based models in the literature.

The method is applied to find the configuration that optimises operational, infrastructure costs as well as service times for the city of London under different demand levels. Results show that UAM systems could effectively be deployed in small scale, with low turnaround times. The findings show that operational costs significantly increase with waiting times, and as such these should be reduced under all circumstances, particularly at higher demand levels. Thus, vertiport design approaches not considering vertiport congestion will lead to suboptimal or infeasible configurations, as was the case with the baseline approach used in this study.

Further work is required to improve the demand modelling to include a logit decision model that considers competing transport modes and multi-modal trips. Moreover, travel times, waiting times, and demand could be modelled stochastically. With the addition of pricing models, these changes would allow the determination of expected profit margins and optimal investment strategies.

CRediT authorship contribution statement

Jose Escribano Macias: Conceptualization and design, Methodology, Software, Analysis, Validation, Writing (Original), Writing (Revision). **Carl Khalife:** Methodology, Software, Analysis, Validation, Writing (Original). **Joseph Slim:** Methodology, Software, Analysis, Validation. **Panagiotis Angeloudis:** Conceptualization and design, Supervision.

Acknowledgements

The research was supported by the UK Engineering and Physical Sciences Research Council (EPSRC), United Kingdom as part of the Sustainable Civil Engineering Centre for Doctoral Training (Grant number EP/L016826/1), the Impact Acceleration Account Funding, United Kingdom (Grant number EP/R511547/1). The study was also supported by InnovateUK as part of the Project 4984.

References

Al Haddad, C., Chaniotakis, E., Straubinger, A., Plötner, K., Antoniou, C., 2020. Factors affecting the adoption and use of urban air mobility. Transp. Res. A 132, 696–712. http://dx.doi.org/10.1016/j.tra.2019.12.020.

Balac, M., Rothfeld, R.L., Horl, S., 2019. The prospects of on-demand urban air mobility in Zurich, Switzerland.

Booz Allen Hamilton, 2018. UAM market study - technical out brief. Technical Report, URL https://ntrs.nasa.gov/search.jsp?R=20190000517.

Brown, A., Harris, W., 2018. A vehicle design and optimization model for on-demand aviation. In: 2018 AIAA/ASCE/AHS/ASC Structures, Structural Dynamics, and Materials Conference. p. 105.

Campbell, J.F., 1996. Hub location and the p-hub median problem. Oper. Res. 44 (6), 923–935. http://dx.doi.org/10.1287/opre.44.6.923.

Chan, W.N., Barmore, B.E., Kibler, J.L., Lee, P.U., O'Connor, C.J., Palopo, K., Thipphavong, D.P., Zelinski, S.J., 2018. Overview of NASA's Air Traffic Management-eXploration (ATM-X) Project.

Chen, L., Wandelt, S., Dai, W., Sun, X., 2021. Scalable vertiport hub location selection for air taxi operations in a metropolitan region. INFORMS J. Comput. (April), 0–23. http://dx.doi.org/10.1287/ijoc.2021.1109.

Chen, H., Yao, D., 2001. Jackson networks, in: Fundamentals of Queueing Networks. Stochastic Modelling and Applied Probability, Vol. 46, pp. 15–35, Springer, New York, NY, http://dx.doi.org/10.1007/978-1-4757-5301-1_2.

Conner, A., Fielden-Page, J., Ranavaya, R., Bailey, L., 2022. Future flight aircraft capabilities. Technical Report, UK Research and Innovation.

Courtin, C., Hansman, R.J., 2019. Model development for a comparison of VTOL and STOL electric aircraft using geometric programming. http://dx.doi.org/10.2514/6.2019-3477.

Daskilewicz, M., German, B., Warren, M., Garrow, L.A., Boddupalli, S.-S., Douthat, T.H., 2018. Progress in vertiport placement and estimating aircraft range requirements for eVTOL daily commuting. In: 2018 Aviation Technology, Integration, and Operations Conference. p. 2884.

Department for Transport Statistics, 2023. National Travel Survey: Travel by household income quintile and main mode / stage mode: England, 2002 onwards.

EASA, 2021. Study on the societal acceptance of urban air mobility in Europe. Technical Report, p. 162.

European Commission, 2021a. Commission implementing regulation (EU) 2021/664 of 22 april 2021 on a regulatory framework for the U-space. pp. 161–183, URL https://eur-lex.europa.eu/eli/reg_impl/2021/664/oj.

European Commission, 2021b. Commission implementing regulation (EU) 2021/665 of 22 april 2021 amending implementing regulation (EU) 2017/373 as regards requirements for providers of air traffic management/air navigation services and other air traffic management network functions in. pp. 184–186, URL http://data.europa.eu/eli/reg_impl/2021/665/oj.

European Commission, 2021c. Commission Implementing Regulation (EU) 2021/666 of 22 April 2021 amending Regulation (EU) No 923/2012 as regards requirements for manned aviation operating in U-space airspace. pp. 187–188, URL http://data.europa.eu/eli/reg_impl/2021/666/oj.

Fixr, 2021. Compare costs estimates.

Fu, M., Straubinger, A., Schaumeier, J., 2020. Scenario-based demand assessment of urban air mobility in the greater Munich area. pp. 1–16. http://dx.doi.org/10.2514/6.2020-3256.

German, B., Daskilewicz, M., Hamilton, T.K., Warren, M.M., 2018. Cargo delivery in by passenger eVTOL aircraft: A case study in the san Francisco Bay Area. In: AIAA SciTech Forum. In: 2018 AIAA Aerospace Sciences Meeting, Kissimmee, FL, USA, http://dx.doi.org/10.2514/6.2018-2006.

Goyal, R., 2018. Urban air mobility (UAM) market study.

Hakimi, L., 1964. Optimum locations of switching centers and the absolute centers and medians of a graph. Oper. Res. 12 (3), 450–459, URL https://www.jstor.org/stable/pdf/168125.pdf.

HM Revenues and Customs, 2018. Carbon emissions tax. Policy Paper, URL https://www.gov.uk/government/publications/carbon-emmisions-tax/carbon-emmisions-tax#detailed-proposal.

Holden, J., Goel, N., 2016. Fast-forwarding to a future of on-demand urban air transportation. URL https://www.uber.com/elevate.pdf.

Holmes, B.J., 2016. A vision and opportunity for transformation of on-demand air mobility. In: 16th AIAA Aviation Technology, Integration, and Operations Conference. p. 3465.

Johnson, W., 2010. NDARC-NASA design and analysis of rotorcraft theoretical basis and architecture. URL http://ntrs.nasa.gov/search.jsp?R=20100021986.

Johnson, W., Silva, C., Solis, E., 2018. Concept vehicles for VTOL air taxi operations. In: Proceedings of the AHS International Technical Meeting on Aeromechanics Design for Transformative Vertical Flight 2018.

Johnston, T., Riedel, R., Sahdev, S., 2020. To take off, flying vehicles first need places to land. Technical Report, McKinsey & Company, Boston, MA, USA.

Kadhiresan, A.R., Duffy, M.J., 2019. Conceptual design and mission analysis for eVTOL urban air mobility flight vehicle configurations. In: AIAA AVIATION Forum. Dallas, TX, USA, pp. 1–19. http://dx.doi.org/10.2514/6.2019-2873.

Klose, A., Drexl, A., 2005. Facility location models for distribution system design. European J. Oper. Res. 162, 4–29. http://dx.doi.org/10.1016/j.ejor.2003.10.031.

Kohlman, L.W., Patterson, M.D., 2018. System-level urban air mobility transportation modeling and determination of energy-related constraints. In: 2018 Aviation Technology, Integration, and Operations Conference, http://dx.doi.org/10.2514/6.2018-3677.

Kohlman, L.W., Patterson, M.D., Raabe, B.E., 2019. Urban air mobility network and vehicle type-modeling and assessment.

Lim, E., Hwang, H., 2019. The selection of vertiport location for on-demand mobility and its application to Seoul Metro Area. Int. J. Aeronaut. Space Sci. 20 (1), 260–272. http://dx.doi.org/10.1007/s42405-018-0117-0.

McDonald, R., German, B., 2017. eVTOL stored energy. In: 2017 Uber Elevate Summit.

Melton, J., Kontinos, D., Grabbe, S., Alonso, J., Sinsay, J., Tracey, B., 2014. Combined electric aircraft and airspace management design for metro-regional public transportation. NASA/TM 216626, 2014.

Ministry of Housing Communities & Local Government, 2020. Land value estimates for policy appraisal 2019. pp. 2019–2021, URL https://www.gov.uk/government/publications/land-value-estimates-for-policy-appraisal-2019.

NASA Urban Air Mobility, 2018. Urban air mobility (UAM) market study. Technical Report, URL https://ntrs.nasa.gov/search.jsp?R=20190026762.

Patterson, M.D., Antcliff, K.R., Kohlman, L.W., 2018. A proposed approach to studying urban air mobility missions including an initial exploration of mission requirements. In: AHS International 74th Annual Forum & Technology Display. Phoenix, AZ.

PowerCompare, 2019. Compare electricity prices: Average UK rates & tariffs per kWh.

Rajendran, S., Zack, J., 2019. Insights on strategic air taxi network infrastructure locations using an iterative constrained clustering approach. Transp. Res. E 128 (July), 470–505. http://dx.doi.org/10.1016/j.tre.2019.06.003.

Rath, S., Chow, J.Y.J., 2019. Air taxi skyport location problem for airport access. arXiv preprint arXiv:1904.01497.

Rothfeld, R., Balac, M., Ploetner, K.O., Antoniou, C., 2018. Initial analysis of urban air mobility's transport performance in sioux falls. In: 2018 Aviation Technology, Integration, and Operations Conference, http://dx.doi.org/10.2514/6.2018-2886.

Silva, C., Johnson, W.R., Solis, E., Patterson, M.D., Antcliff, K.R., 2018. VTOL urban air mobility concept vehicles for technology development. In: 2018 Aviation Technology, Integration, and Operations Conference. p. 3847.

Sinha, A.A., Rajendran, S., 2022. A novel two-phase location analytics model for determining operating station locations of emerging air taxi services. Decis. Anal. J. 2 (June 2021), 100013. http://dx.doi.org/10.1016/j.dajour.2021.100013.

Sinsay, J., Alonso, J., Kontinos, D., Melton, J., Grabbe, S., 2012. Air vehicle design and technology considerations for an electric VTOL metro-regional public transportation system. In: 12th AIAA Aviation Technology, Integration, and Operations (ATIO) Conference and 14th AIAA/ISSMO Multidisciplinary Analysis and Optimization Conference. p. 5404.

Taylor, M., Saldanli, A., Park, A., 2020. Analysis of alternate vertiport designs. In: Proceedings IEEE ICNS Conference. IEEE, Dulles, Virginia.

Transport for London, 2019. TfL rolling origin and destination survey.

Turner & Townsend, 2015. International construction market survey 2016. In: Global Rebalancing: A Changing Landscape. pp. 1–76.

Uber, 2018. eVTOL vehicle requirements and missions. URL https://s3.amazonaws.com/uber-static/elevate/Summary+Mission+and+Requirements.pdf.

Wang, Z., Alam, S., Delahaye, D., Farges, J.-L., 2022. Route network design in low-altitude airspace for future urban air mobility operations-a case study of urban airspace of Singapore data-driven 4D trajectory prediction view project proteus view project route network design in low-altitude airspace for fut. In: International Conference on Research in Air Transportation, 19th ed. Tampa, Florida, US, URL https://www.researchgate.net/publication/361584773.

Wang, Z., Delahaye, D., Farges, J.L., Alam, S., 2023. A quasi-dynamic air traffic assignment model for mitigating air traffic complexity and congestion for high-density UAM operations. Transp. Res. C 154, http://dx.doi.org/10.1016/j.trc.2023.104279.

Wei, L., Justin, C.Y., Mavris, D.N., 2020. Optimal placement of airparks for STOL urban and suburban air mobility. In: AIAA SciTech Forum. Orlando, FL, USA, pp. 1–16. http://dx.doi.org/10.2514/6.2020-0976.

Willey, L.C., Salmon, J.L., 2021. A method for urban air mobility network design using hub location and subgraph isomorphism. Transp. Res. C 125 (May 2020), 102997. http://dx.doi.org/10.1016/j.trc.2021.102997.

Wu, Z., 2020. Exploration of on-demand urban air mobility: Network design, operation scheduling and uncertainty considerations. pp. 1–4.

Wu, Z., Zhang, Y., 2021. Integrated network design and demand forecast for on-demand urban air mobility. Engineering 7 (4), 473–487. http://dx.doi.org/10.1016/j.eng.2020.11.007.